Available online at www.sciencedirect.com
ScienceDirect
Trans. Nonferrous Met. Soc. China 25(2015) 3048−3055
Transactions of Nonferrous Metals Society of China
www.tnmsc.cn

Constitutive modeling and springback simulation for 2524 aluminum alloy in creep age forming

You-liang YANG[1,2], Li-hua ZHAN[1,2], Jie LI[2,3]

1. State Key Laboratory of High-performance Complex Manufacturing, Central South University, Changsha 410083, China;
2. School of Mechanical and Electrical Engineering, Central South University, Changsha 410083, China;
3. Changsha Engineering & Research Institute Ltd. of Nonferrous Metallurgy, Changsha 410011, China

Received 13 October 2014; accepted 23 April 2015

Abstract: The constitutive modeling and springback simulation for AA2524 sheet in creep age forming (CAF) process were presented. A series of creep aging tests were performed on AA2524 at the temperature of 180−200 °C and under the stress of 140−210 MPa for 16 h. Based on these experimental data, material constitutive equations which can well characterize creep aging behaviors of the tested alloy were developed. The effect of interior stress distributed along the sheet thickness on springback was simulated using FE software MSC. MARC by compiling the established constitutive models into the user subroutine. The simulation results showed that the amount of sheet springback was 61.12% when merely considering tensile stress existing along the sheet thickness; while sheet springback was up to 65.93% when taking both tensile and compressive stresses into account. In addition, an AA2524 rectangular sheet was subjected to CAF experiment in resistance furnace. The springback value of the formed rectangular sheet was 68.2%, which was much closer to 65.93%. This confirms that both tensile and compressive stresses across the sheet thickness should be considered in accurately predicting springback of the sheet after forming, which can be more consistent with experimental results.

Key words: 2524 aluminum alloy; creep age forming; constitutive modeling; springback simulation; stress state

1 Introduction

In recent years, there have been increasing demands in aerospace industry for manufacturing better performance aircraft integral panels with improved strength and toughness, heightened resistance to fatigue and corrosion [1−4]. However, forming of large integral panels by conventional metal forming methods shows relatively high levels of residual stress in the formed parts, which easily initiate fatigue and stress corrosion cracking. Therefore, creep age forming (CAF), a favored forming process which combines creep deformation and age-hardening, is explored [5−8].

Constitutive modelling and springback prediction are two main aspects required to research CAF process. HO et al [3] used a set of creep damage constitutive equations for CAF springback simulation. The results indicated that creep mainly took place near the top and bottom surfaces of the workpiece and the amount of springback can be assessed by the ratio of "significant creep region" (SCR) and "less creep region" (LCR). ZHAN et al [6] formulated a mechanism-based unified creep aging constitutive equation set. With this equation set, springback of the formed part was also simulated. HUANG et al [9] developed creep constitutive equations for 7050 aluminum alloy and studied the effect of the forming parameters on the springback of AA7050 plate. JEUNECHAMPS et al [10] built constitutive models by the unified theory and programmed efficient numerical techniques and procedures to predict springback in CAF process. They found that the amount of springback decreased almost linearly as the curvature of the workpiece varied from single curvature to double curvature. LIN et al [11] proposed a new constitutive model based on the Bailey−Norton law and θ projection method that shows a good agreement between the predicted and measured creep strains. However, these

Foundation item: Project (2014CB046602) supported by the National Basic Research Program of China; Project (20120162110003) supported by PhD Programs Foundation of Ministry of Education of China
Corresponding author: Li-hua ZHAN; Tel: +86-731-88830254; E-mail: yjs-cast@csu.edu.cn
DOI: 10.1016/S1003-6326(15)63932-2

constitutive models are established merely based on tensile tests and corresponding springback simulation results cannot be in good agreement with practical springback of sheet, as both tensile and compressive stresses occur along the sheet thickness direction in the practical CAF process.

In this work, two sets of constitutive models respectively describing tensile creep behavior and compressive creep behavior of AA2524 were derived; the effect of interior stress distributed along the sheet thickness direction on springback was simulated using FE software MSC. MARC by compiling the established constitutive models into the user subroutine; CAF test was carried out on an AA2524 rectangular sheet and the springback values between simulated and experimental were compared and analyzed.

2 Experimental

The studied materials were obtained from a company as hot-rolled plates of AA2524. The exact chemical composition is given in Table 1. Tensile specimens of 3.5 mm in thickness and cylindrical compression specimens of 10 mm in height and 5 mm in diameter were machined out from the rolling direction of as-received plates, as illustrated in Fig. 1. Solid solution treatments were conducted in resistance furnace at potentiometer-controlled temperature of (498±3) °C for 52 min for tensile specimens and 65 min for compression ones. Subsequently, the specimens were kept in a refrigerated condition to reduce natural aging.

Uniaxial tensile and compressive creep tests were carried out on specimens at 180, 190 and 200 °C under the stress of 140, 180, 190 and 210 MPa for 16 h, respectively. The specimen was fitted and aligned in the middle of the furnace. Then the furnace was closed and heated. When the temperature in the furnace reached the goal value and became steady for about 10 min, the extensometers were calibrated and the pre-selected load was applied. The test was ceased after 16 h and the specimen was naturally cooled to the room temperature in the furnace.

3 Establishment of material models

3.1 Creep behaviors of AA2524

Figure 2 depicts the creep curves of the specimens under tested conditions. It is observed that the creep curves are almost in the first two creep stages with the exception of the curves tested under 210 MPa in compression because there is tertiary creep at the end of test. It is also seen that the creep strains in compression are roughly twice than that in tension. For example, under the condition of 190 MPa, 16 h and 190 °C, the compressive creep strain is 0.24% while the tensile creep strain is 0.113%. Furthermore, the creep strain whether in compression or tension is in direct proportion to aging time, temperature and stress level, which is consistent with Refs. [11,12].

3.2 Constitutive equation for AA2524 creep-aged in tension

SODERBERG [13] constructed accumulation theory of strain, in which the creep strain is related to applied stress and aging time at a certain temperature. It is expressed as

$$\varepsilon = f(\sigma, t) \tag{1}$$

where ε, σ and t represent creep strain, applied stress and aging time, respectively. As seen from Fig. 2, aging temperature is an important factor that influences the creep strain. Thus, the contribution of aging temperature to creep strain is coupled as

$$\varepsilon = f(\sigma, t, T) \tag{2}$$

where T refers to aging temperature. For the metal

Table 1 Chemical composition of AA2524 (mass fraction, %)

Cu	Mg	Mn	Fe	Zn	Ti	Cr	Si	Zr	Ni	Al
4.26	1.36	0.57	0.037	0.024	0.01	0.002	0.089	0.001	0.001	Bal.

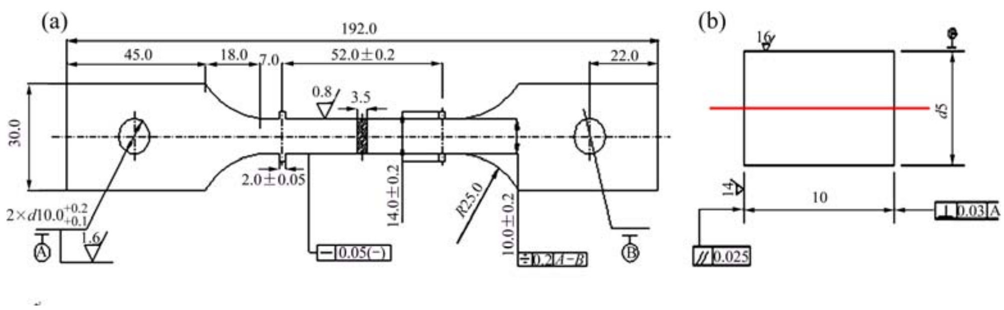

Fig. 1 Geometry of tensile specimen (a) and compression specimen (b) (unit: mm)

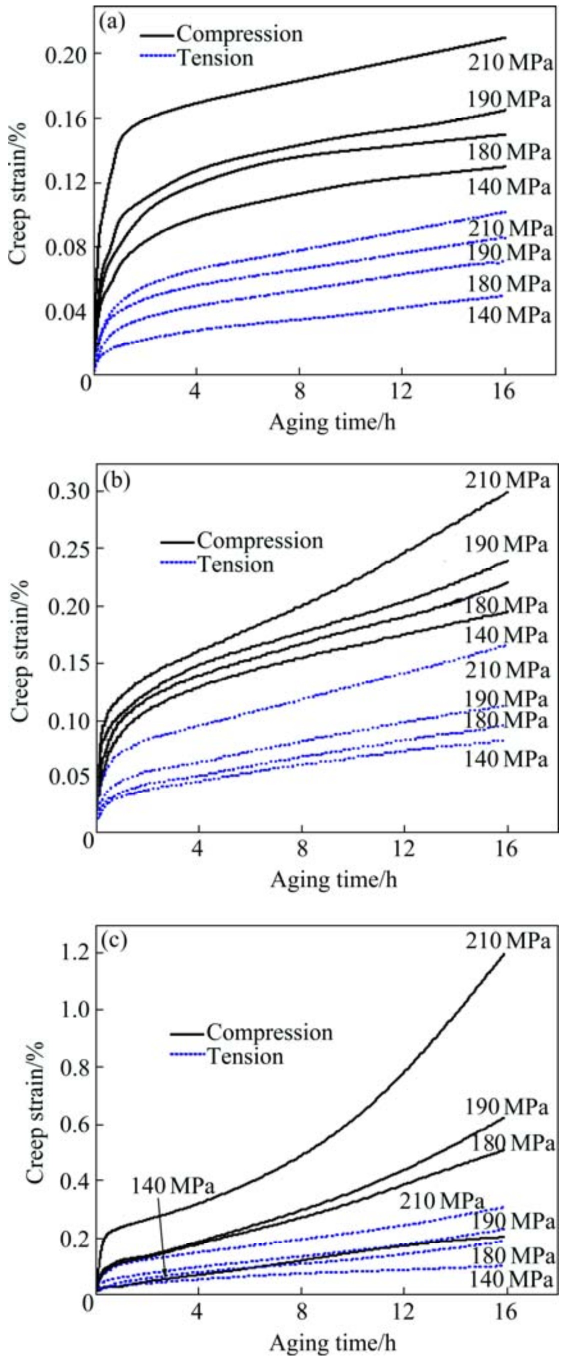

Fig. 2 Creep strain−aging time curves of specimens at temperatures of 180 °C (a), 190 °C (b), and 200℃ (c)

material, creep curves have geometric similarity in the first and the second stages [14], Eq. (2) can be simplified to the following form:

$$\varepsilon = f(\sigma) f(t) f(T) \tag{3}$$

where $f(\sigma)$, $f(t)$ and $f(T)$ respectively denote stress function, aging time function and temperature function. According to precipitation hardening, dislocation hardening and thermal softening, Eq. (3) is expanded as [15]

$$\varepsilon = A(\sigma - \sigma_0)^n (t^m + Ct) \exp[-Q/(RT) + D] \tag{4}$$

where A, σ_0, n, m, C, and D are material constants, R is the mole gas constant, Q is the creep activation energy.

Equation (4) is developed with the following considerations. The first term, $A(\sigma-\sigma_0)^n$, represents the combined effects of externally applied stress and internal stress. The internal stress, σ_0, is introduced to the model due to precipitation strengthening caused by precipitated phases. The stress sensitivity is controlled by the exponent, n, which is between 2 and 10 for metals and alloys. For the second term, it reveals the effect of aging time. The creep strain related to aging time in the primary creep stage is defined by power function of t^m. Material constant, m, lies within the range from 0 to 1. Meanwhile, Ct is linearly responsible for the creep strain in the secondary creep stage. These characteristics are clearly seen in Fig. 2. The last term gives the influence of temperature or thermal softening in throughout creep aging process. On one hand, it is generally believed that creep is a thermal-activated process which is sensitive to the variation of temperature. On the other hand, due to the slight fluctuation of temperature in CAF process, a parameter, D, is employed to improve the effectiveness of model. Considering above two reasons, the final term, $\exp[-Q/(RT)+D]$ is integrated in Eq. (4).

3.3 Constitutive equations for AA2524 creep-aged in compression

With regard to Fig. 2, some compressive creep curves are in the tertiary creep stage. In this case, the general constitutive models reflecting the primary and secondary creep stages are not suitable for this condition. Based on continuum damage mechanics, KOWALEWSKI et al [16] presented physically-based unified creep constitutive equations with three state variables in sinh function to model primary creep hardening and tertiary creep softening in aluminum alloys by mechanisms of 1) dislocation hardening at the initial stage of creep, 2) aging softening at high temperature, and 3) softening due to grain cavity nucleation and growth. For the precise characterization of AA2524 creep-aged in compression, the equations enabling the primary, secondary, and tertiary creep to be captured are adopted and listed below [16]:

$$\dot{\varepsilon} = [A/(1-\omega_2)^n] \sinh[B\sigma(1-H)/(1-\phi)] \tag{5}$$

$$\dot{H} = (h/\sigma)(1 - H/H^*)\dot{\varepsilon} \tag{6}$$

$$\dot{\phi} = (k_c/3)(1-\phi)^4 \tag{7}$$

$$\dot{\omega}_2 = D\dot{\varepsilon} \tag{8}$$

where A, B, h, k_c, H^*, and D are materials constants, and n is given by

$$n=[B\sigma(1-H)/(1-\phi)]\coth[B\sigma(1-H)/(1-\phi)] \tag{9}$$

Equation (5) refers to evolution of creep strain. The material constants A and B characterize secondary creep. Primary creep is defined by using hardening state variable, H, which varies from 0 at the beginning of creep process to H^*, the saturation value of H at the end of primary creep and subsequently maintains this value for the remaining of the creep deformations. The tertiary creep is defined by the two variables ϕ and w_2.

3.4 Determination of material constants

The determination of the material constants involved in the constitutive equations is carried out by the experimental data and the use of particle swarm optimization algorithm. Through this algorithm, the material constants within Eqs. (4)−(9) are confirmed and listed in Tables 2 and 3, respectively.

Comparisons of predicted and experimental data are made and shown in Fig. 3. It can be seen that computed creep strains are in good agreement with experimental values for selected stress levels, indicating that the established constitutive equations have strong capacity to model creep aging behaviors.

4 Finite element simulation for springback in CAF process

In general, material constants within constitutive model are identified using the experimental data from uniaxial tensile or compressive creep age tests. Then, the springback of the formed component is simulated by integrating the constitutive equations into finite element solver. In such case, only one stress mode (tension or compression) is involved in simulating the springback of sheet in CAF process. However, once the sheet is pressed by mechanical load or vacuum bagging technique and contacts with cylinder surface of die, stress distribution along the sheet thickness varies from compression on the upper surface of the sheet to tension on the lower surface (see Fig. 4), reaching maximum value on the outer surfaces of the sheet. Consequently, the aim of this part is to study the effect of stress modes (tension and

Table 2 Material constants within tensile constitutive equation (Eq. (4))

A	σ_0	n	m	C	D	Q	Determination coefficient, R^2
1×10^{-9}	28.04	2	0.3164	0.036	37.75	97855	0.9753

Table 3 Materials constants within compressive constitutive equation (Eqs. (5)−(9))

Temperature/°C	A	B	h	H^*	k_c	D	Determination coefficient, R^2
180	5.0×10^{-6}	0.0725	1018.26	0.6289	1.0×10^{-6}	−4.174	0.9681
190	6.15×10^{-6}	0.0715	−9.64	0.00212	6.867×10^{-4}	−3.691	0.9855
200	9.61×10^{-6}	0.0667	977.939	0.3456	5.826×10^{-4}	0.09592	0.9892

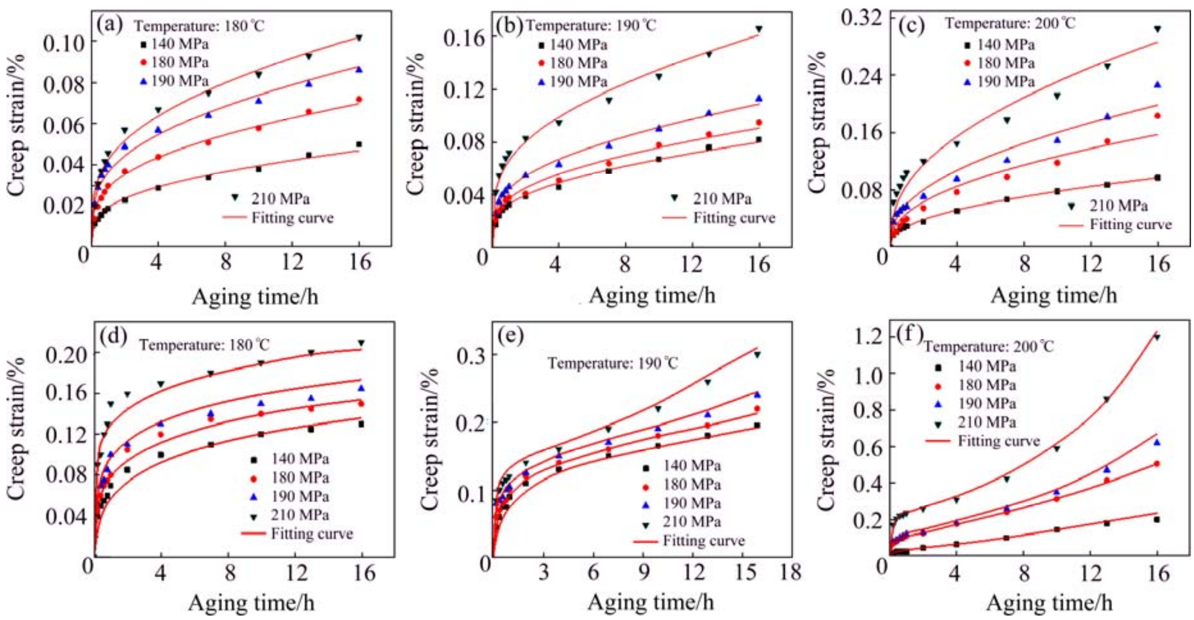

Fig. 3 Comparisons of predicted and experimental creep strains of 2524 aluminum alloy at temperatures of 180 °C (a, d), 190 °C (b, e), and 200 °C (c, f): (a, b, c) Tensile creep-aged tests; (d, e, f) Compressive creep-aged tests

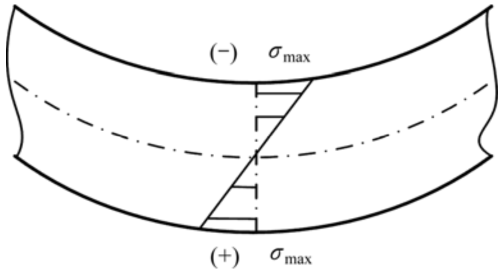

Fig. 4 Distribution of stress along sheet thickness in creep age forming process

compression) on the amount of springback in CAF process by means of finite element simulation.

It is required to compile the constitutive equation as subroutine and put it into software to simulate creep age forming process. For the purpose of comparison, two subroutines are programmed by the Fortran language. One is based on the established "uniaxial tensile constitutive equation" (UTCE), which only involves tensile state; the other is based on the "combination of tensile and compressive constitutive equations" (CTCCE), which considers stress states of tension and compression synchronously.

4.1 Finite element model and simulation procedures

A finite element model was created to simulate creep age forming process using FE software MSC. MARC，the schematic diagram is provided in Fig. 5. The rectangular sheet had the dimensions of 300 mm × 80 mm × 3.5 mm. The single curvature radius of die surface was 1000 mm. Four springs at the each corner of sheet were applied to supporting the weight of the panel. Friction coefficient between the sheet and tool surface was taken as 0.3. The temperature dependence of elastic module of material was determined to be 69.2 GPa at 180 °C. Poisson ratio was set as 0.3. The four-node quadrangular 3D-shell element was used for the analysis. Last, the subroutine was integrated into finite element solver. To simplify the simulation process, the swelling phenomena existing in tool and workpiece in CAF process were ignored.

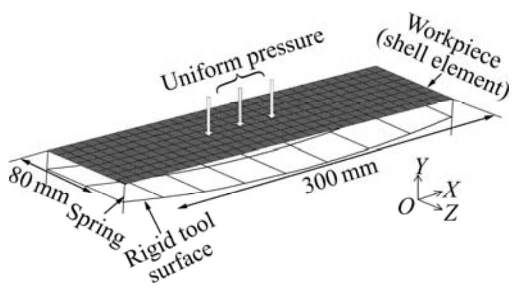

Fig. 5 Finite element model with boundary and loading conditions

The specific procedures for finite element simulation of sheet in creep age forming are summarized as below:

Step 1: Apply uniform pressure to deforming the panel against the tool surface completely (In experimental process, multiple cylindrical indenters are used to press plate to contact with die surface).

Step 2: Maintain the pressure to hold the sheet on the tool surface for a controlled time, for example, 12 h in this study.

Step 3: Release the pressure and allow the aluminum panel to springback. Collect panel data for springback calculation.

Figure 6 exhibits the schematic diagram for springback definition, which is expressed by

$$S(\delta)=(1-\delta_{\rm f}/\delta_0)\times100\% \qquad (10)$$

where $S(\delta)$ denotes the amount of springback, δ_0 and $\delta_{\rm f}$ represent the deflection at the centre of the sheet before and after the pressure is released.

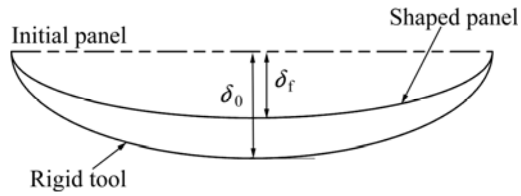

Fig. 6 Schematic diagram for springback definition

4.2 Computational results

Figure 7 illustrates the equivalent von Mises stress (MPa) of upper surface of panel in CAF process. Figures 7(a), (c) and (e) denote the stress distribution of sheet simulated by UTCE and Figs. 7(b), (d) and (f) represent that simulated by CTCCE. For the initial loading, the uniform pressure deformed the panel against the tool surface completely. At this stage, the maximum effective stress in Fig. 7(a) was the same as that in Fig. 7(b), with a value of about 130.4 MPa, which was well below the yield strength (252.3 MPa). This indicates that creep strain occurred at an elastic level. During the aging time, interior stresses produced by forming were relaxed gradually due to creep. Maximum equivalent stress was decreased from 130.4 to 61.59 MPa in Fig. 7(c) and from 130.4 to 69.19 MPa in Fig. 7(d). Figures 7(e) and (f) display the residual stress after springback.

In y-axis direction, displacement distribution of the panel after unloading was computed in Fig. 8. It is observed that the displacement in the centre region was relatively large. But the displacement in Fig. 8(a) was a little greater than that in Fig. 8(b). The displacements of five points on the left of the panel (see Fig. 9) were collected and listed in Table 4. As seen from Table 4, the

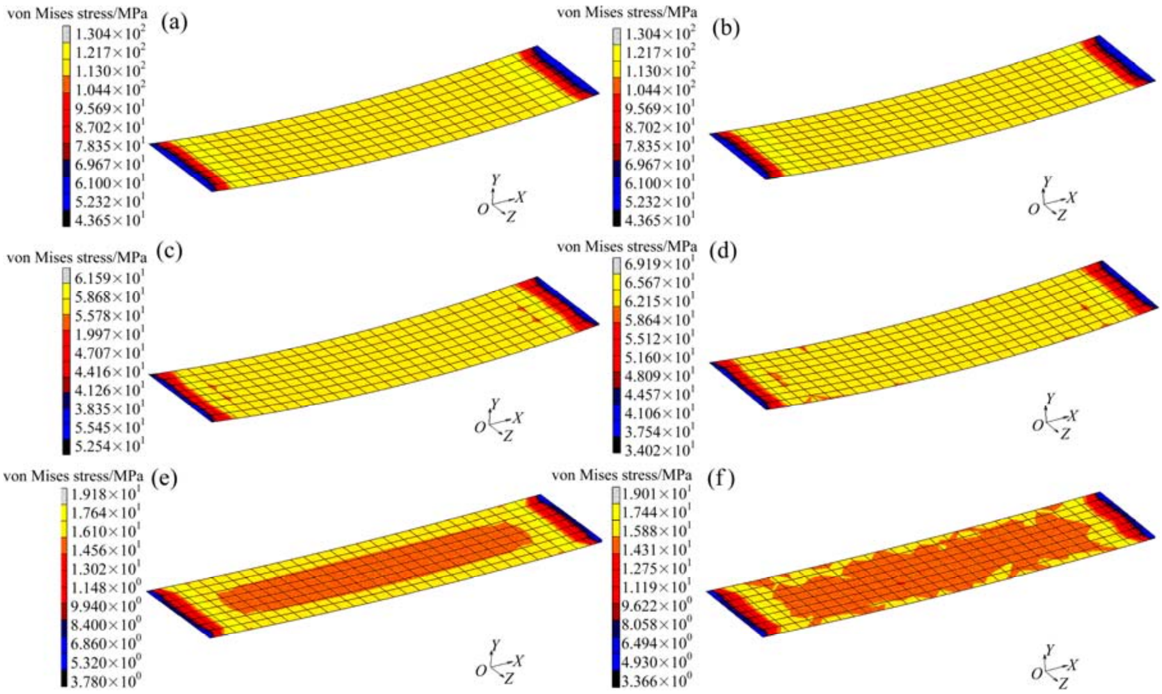

Fig. 7 von Mises stress distribution of sheet during forming process simulated by UTCE (a, c, e) and CTCCE (b, d, f): (a, b) Deformed to its target shape (t=0.1 h); (c, d) Held for 12 h (t=12.1 h); (e, f): After unloading (t=12.11 h)

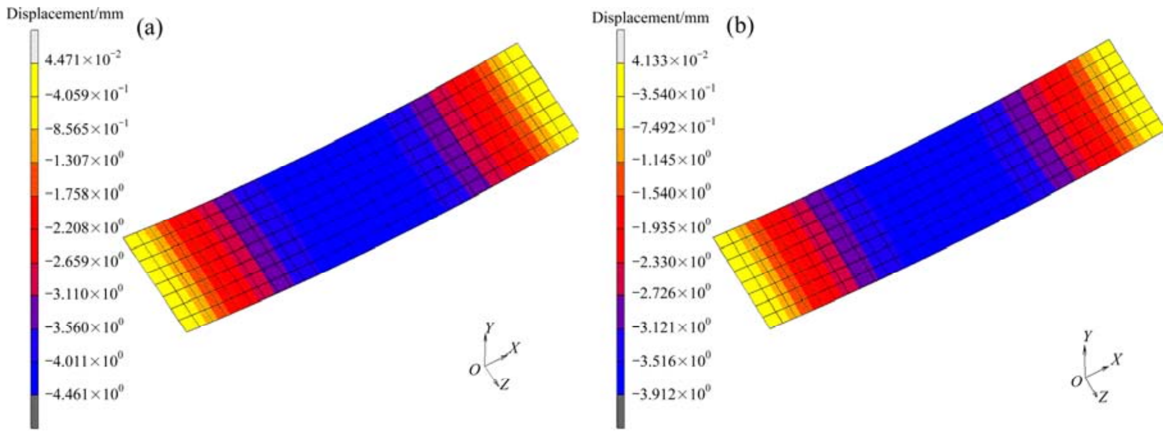

Fig. 8 Displacement distribution of panel after unloading: (a) Simulated by UTCE; (b) Simulated by CTCCE

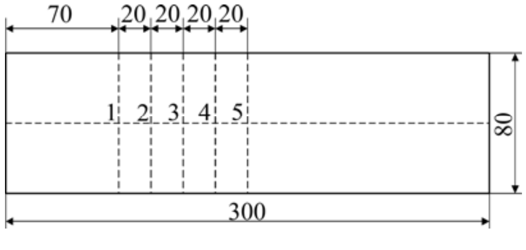

Fig. 9 Five points in upper surface for measuring average value of springback (unit: mm)

average values of springback simulated by UTCE and CTCCE were 61.12% and 65.93%, respectively.

4.3 Experimental verification

Creep age forming test was performed on a 300 mm×80 mm×3.5 mm AA2524 plate using the toolset as illustrated in Fig. 10. Multiple cylindrical indenters were used to press the plate to contact with die surface. The test parameters were totally identical to those defined in the simulation, i.e., 180 °C, 12 h and 1000 mm.

Table 5 gives the experimental springback values of five points on the panel upper surface. With respect to Table 5, springback decreased slightly with the increasing point from 1 to 5. This provides an indication that more stress was relaxed and more creep strain was

Table 4 Data of five points on upper surface of panel and their springback

Point	Initial deflection, δ_0/mm	Final deflection simulated by UTCE, δ_f/mm	Final deflection simulated by CTCCE, δ_f/mm	Springback simulated by UTCE/%	Springback simulated by CTCCE/%
1	8.11	3.14115	2.75265	61.27	66.06
2	9.5113	3.69493	3.23799	61.15	65.96
3	10.5127	4.09059	3.58461	61.09	65.90
4	11.1137	4.32803	3.79256	61.06	65.87
5	11.314	4.40718	3.86172	61.05	65.87
Average	−	−	−	61.12	65.93

Fig. 10 Toolset for creep age forming

Table 5 Amount of springback calculated by experimental data

Point	Initial deflection, δ_0/mm	Final deflection, δ_f/mm	Experimental springback/%
1	8.11	2.57	68.31
2	9.51	3.02	68.24
3	10.51	3.34	68.22
4	11.11	3.54	68.14
5	11.31	3.61	68.08
Average	−	−	68.20

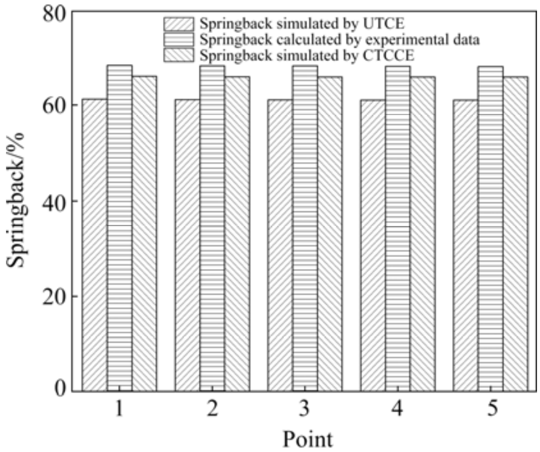

Fig. 11 Comparisons of springback values obtained by simulation and experiment

retained in centre area of the plate. In addition, it is obvious that the experimental springback values of the formed plate are between 68.08%−68.31%, with an average value of 68.20%, which is higher than those simulated by UTCE and CTCCE. Figure 11 presents the comparisons of measured and simulated springback results. It is clear from Fig. 11 that the springback values simulated by CTCCE are closer to experimental results. This experimentally demonstrates that both tensile and compressive stress should be considered in precisely predicting the springback, because it is much closer to the actual result.

In the practical CAF process, the interior stresses distribute linearly from compression on the upper surface of the plate to tension on the lower surface (see Fig. 4). While the creep deformation mechanism is different under tension and compression. In this work, the average stress exponents for tensile creep and compression creep are 3.38 and 2.78, respectively, which are both close to 3. This indicates that the main tensile creep deformation mechanism is dislocation slip companied by a little grain boundary slip; compressive creep deformation mechanism is principally controlled by grain boundary slip along with slight dislocation slip. The different creep deformation mechanisms lead to different deformation of CAF-treated plate and finally to different springback values. Consequently, it is not advisable to take only single uniaxial stress (tension or compression) into account in predicting springback of plate.

5 Conclusions

1) Two sets of constitutive equations which can respectively describe tensile creep behaviors and compressive creep behaviors of AA2524 are derived.

2) The effect of stress states along sheet thickness direction on springback of sheet is simulated. The simulation results show that the amount of springback of sheet is 61.12% when merely considering tensile stress existing along the sheet thickness; while sheet springback is up to 65.93% when taking both tensile and compressive stresses into account.

3) An AA2524 rectangular sheet is subjected to

CAF experiment in resistance furnace. The springback value of the formed rectangular sheet is 68.2%, which is much closer to 65.93%. This confirms that both tensile and compressive stresses across the sheet thickness should be considered in accurately predicting springback of the sheet after forming, because it can be more consistent with experimental results.

References

[1] LAMA A C L, SHI Z S, YANG H L, WAN L, DAVIES C, LIN J G, ZHOU S J. Creep-age forming AA2219 plates with different stiffener designs and pre-form age conditions: Experimental and finite element studies [J]. Journal of Materials Processing Technology, 2014, 219: 155−163.

[2] HO K C, LIN J, DEAN T A. Constitutive modelling of primary creep for age forming an aluminium alloy [J]. Journal of Materials Processing Technology, 2004, 153: 122−127.

[3] HO K C, LIN J, DEAN T A. Modelling of springback in creep forming thick aluminum sheets [J]. International Journal of Plasticity, 2004, 20(4−5): 733−751.

[4] PITCHER P D, STYLES C M. Creep age forming of 2024A, 8090 and 7449 alloys [J]. Materials Science Forum, 2000, 331−337: 455−460.

[5] ZHAN L H, LIN J, DEAN T A. A review of the development of creep age forming: Experimentation, modelling and applications [J]. International Journal of Machine Tools & Manufacture, 2011, 51(1): 1−17.

[6] ZHAN L H, LIN J G, DEAN T A, HUANG M H. Experimental studies and constitutive modelling of the hardening of aluminium alloy 7055 under creep age forming conditions [J]. International Journal of Mechanical Sciences, 2011, 53(8): 595−605.

[7] ZHAN Jin, DENG Yun-lai, LI Si-yu, CHEN Ze-yu, ZHANG Xin-ming. Creep age forming of 2124 aluminum alloy with single/double curvature [J]. Transactions of Nonferrous Metals Society of China, 2013, 23(7): 1922−1929.

[8] QUAN Li-wen, ZHAO Gang, TIAN Ni, HUANG Ming-li. Effect of stress on microstructures of creep-aged 2524 alloy [J]. Transactions of Nonferrous Metals Society of China, 2013, 23(8): 2209−2214.

[9] HUANG X, ZENG Y S, GAI P T. Experimental studies and FEM analysis on the creep age forming for aluminium alloy 7050 [J]. Materials Science Forum, 2013, 773−774: 144−152.

[10] JEUNECHAMPS P P, HO K C, LIN J, PONTHOT J P, DEAN T A. A closed form technique to predict springback in creep age-forming [J]. International Journal of Mechanical Sciences, 2006, 48(6): 621−629.

[11] LIN Y C, JIANG Y Q, ZHOU H M, LIU G. A new creep constitutive model for 7075 aluminum alloy under elevated temperatures [J]. 2014, 23 (12): 4350−4357.

[12] JESHVAHANI R A, EMAMI M, SHAHVERDI H, HADAVI S. Effects of time and temperature on the creep forming of 7075 aluminum alloy: Springback and mechanical properties [J]. Materials Science and Engineering A, 2011, 528 (29−30): 8795−8799.

[13] SODERBERG C R. The interpretation of creep tests for machine design [J]. Trans ASME, 1936, 58: 733−743.

[14] GLADMAN T. Precipitation hardening in metals [J]. Materials Science and Technology, 1999, 15: 30−36.

[15] LI Yan-guang. Experimental study and constitutive modeling on creep aging for 2124 aluminum alloy [D]. Changsha: Central South University, 2012: 56−58. (in Chinese)

[16] KOWALEWSKI Z, HAYHURST D, DYSON B. Mechanisms-based creep constitutive equations for an aluminium alloy [J]. The Journal of Strain Analysis for Engineering Design, 1994, 29: 309−316.

2524 铝合金蠕变时效本构建模及回弹仿真

杨有良[1,2], 湛利华[1,2], 李 杰[2,3]

1. 中南大学 国家高性能复杂制造重点实验室，长沙 410083；

2. 中南大学 机电工程学院，长沙 410083；

3. 长沙有色金属设计研究院，长沙 410011

摘 要：研究 2524 铝合金板材蠕变时效过程中的本构建模及回弹仿真。在 180~200 ℃、140~210 MPa 和 16 h 条件下，对 2524 铝合金进行一系列的蠕变时效实验。基于这些实验数据建立能够很好地描述合金蠕变时效行为的材料本构模型。通过将本构模型嵌入到有限元软件 MSC.MARC 的子程序中，分析沿板材厚度分布的内应力对回弹的影响。仿真结果表明：仅考虑拉应力时，板材回弹量为 61.12%，而同时考虑拉应力和压应力时，回弹量为 65.93%。另外，对 2524 铝合金板材进行蠕变时效成形实验。成形板材回弹量为 68.2%，其值更接近 65.93%。这表明仿真分析时同时考虑板材厚度方向的拉压内应力更能准确预测构件的回弹量，这样得到的仿真结果更符合实验结果。

关键词：2524 铝合金；蠕变时效成形；本构建模；回弹仿真；应力状态

(Edited by Yun-bin HE)